

tion of the ESO Schmidt telescope at La Silla, in 1972. Part of this work was done in collaboration with the UK Schmidt telescope in Australia.

In 1980, Caltech astronomers began planning for a new, northern survey because of advances in photographic and telescope technology and the changes in the heavens over the ensuing three decades. The Oschin Telescope was substantially refurbished before the second sky survey was begun. This included a new, \$380,000 lens that enables the telescope to focus a wide range of wavelengths. In addition, advances in photographic technology have led to the development of photo-

graphic plates that are far more sensitive than those available in 1948.

Each glass plate is 14 inches square, and photographs a segment of the sky about 6.5 degrees across, about 13 times the diameter of the full moon. It would take 894 such segments to cover the entire northern hemisphere of the sky, but since each segment is photographed at three wavelengths, the survey will finally comprise 2,682 plates. Because of the trails of overflying airplanes, plate defects, or other observational problems, the Caltech astronomers expect that they will have to expose two plates for every one that is finally accepted for the survey.

Orders for the new Atlas should be sent to the ESO Information Service, Karl-Schwarzschild-Straße 2, D-8046 Garching bei München, Federal Republic of Germany.

The cost of one atlas (894 copies each in B, R and I; in total 2,682 copies) is DM 60,000 on film and DM 460,000 on glass, if prepaid. It is also possible to pay before each shipment; in this case an inflation variation will be applied and it is expected that about one-tenth to one-eighth of the total price will be called up each year. Reservations can be made until July 1, 1990.

(From ESO Press Release 2/90)

Near-Ground Seeing on an Interferometric Platform

L. ZAGO, ESO

1. Introduction

The ideal location for an optical telescope, short of being in orbit, would be being magically suspended in the air, out of all ground-induced turbulence. Most observatories try the next best, a location on a steep peak or ridge, in the generally correct assumption that the abrupt rising of the mountain does not give the air flow the time and space to bring ground-induced turbulence on the telescope.

An interferometric observatory, however, which is made of several, possibly mobile, telescopes, will need a much larger flat space than is usually the case for a single telescope. This is in particular the case for the VLT, which requires a large and rather flat platform of the order of 180 × 150 m to accommodate the four main unit telescopes, the optical laboratories and the tracks for the smaller auxiliary telescopes. One may then fear that telescopes located at some distance from the edge of the platform will have their seeing affected by turbulence created along the stretch of flat surface upwind.

The purpose of this article is to describe a simplified model of the near-ground seeing phenomenon aimed at identifying the main influencing parameters and the order of magnitude of their effects.

2. A Simplified C_T^2 Model

The temperature structure coefficient C_T^2 is the local parameter which most suitably represents the optical quality of an atmospheric layer. The local C_T^2 can

in principle be expressed in terms of bulk parameters of the atmosphere, such as temperature, pressure, wind velocity and their derivatives. However, a rigorous formulation will generally be very complex for any non-trivial aerodynamic field and the calculation of C_T^2 will require a finite element or difference scheme.

Therefore we will take here some simplifying assumptions in order to derive a simple analytical formulation, which at the price of some quantitative accuracy, yet allows to identify the physical quantities influencing the seeing phenomenon and obtain useful comparative data for different situations.

We start from the relationship of C_T^2 with dissipation rates:

$$C_T^2 = a^2 \varepsilon_\theta \varepsilon^{-\frac{1}{3}} \quad (1)$$

Neglecting transport in the longitudinal and transversal direction and under conditions of stationary turbulence, the dissipation rates can be expressed as:

$$\begin{aligned} \varepsilon_\theta &= K_H \left(\frac{d\theta}{dz} \right)^2; \\ \varepsilon &= K_m \left(\frac{dU}{dz} \right)^2 - K_H \frac{g}{\theta} \frac{d\theta}{dz} \end{aligned} \quad (2)$$

For K_H we take here the expression valid for a stationary boundary layer (K_m is then assumed equal to $K_H/1.35$):

$$K_H = k^2 z^2 \left| \frac{dU}{dz} \right| \quad (3)$$

In this way C_T^2 is expressed in terms of the vertical temperature and velocity profiles only. One should note that the velocity gradient represents here a scale of the mechanical turbulence: indeed for a stationary boundary layer, the turbulent velocity σ_u (rms of velocity fluctuations) is directly related to the velocity gradient through the friction velocity u_* .

$$\frac{dU}{dz} = \frac{u_*}{kz} = \frac{\sigma_u}{z} \quad (4)$$

Note also that temperature and velocity are not properly independent variables, as the temperature gradient is linked through K_H to the velocity turbulence by the heat flux equation:

$$q(z) = K_H \frac{d\theta}{dz} = k^2 z^2 \left| \frac{dU}{dz} \right| \frac{d\theta}{dz} \quad (5)$$

The local flux $q(z)$ is generally a function of the surface-air heat flux q_s , which depends on thermal ground characteristics, solar irradiation and also on wind turbulence as a more turbulent flow will

List of symbols

<p>ε_θ = dissipation rate of temperature variance. ε = dissipation rate of turbulent kinetic energy. a^2 = a constant equal to about 3. θ = potential temperature. z = height above ground. U = wind mean velocity. σ_u = wind turbulent velocity. u_* = flow friction velocity. K_H = eddy diffusivity for heat. K_m = eddy diffusivity for momentum. k = von Karman's constant = 0.4. g = gravity acceleration. $q(z)$ = local vertical heat flux. q_s = air-ground heat flux.</p>
--

exchange more heat with the ground. For the purpose of parametric evaluation, one can assume the following proportionality:

$$q(z) \propto q_s \propto \frac{u_*^2}{U} \quad (6)$$

One can now use expressions (1) to (6) to compute and compare the seeing of different situations. As a reference case, we shall take a "good seeing" situation for an optimal location on the mountain, that is on the windward edge of the mountain ridge, with the following conditions:

- Mean wind velocity $U = 10$ m/s.
- Turbulent velocity $\sigma_u = 0.75$ m/s. Note that measured values of wind turbulence at any given mean velocity are quite scattered: at Paranal, for instance, for a mean of 10 m/s, the rms may range from 0.4 to 1.4 m/s. We then use expression (4) to get an estimate of the local velocity gradient and evaluate K_H from (3).

- The vertical heat flux is more difficult to estimate. We will assume here a value of 0.009 K m/s: note, for reference, that on a large plain the night-time surface heat flux can be of the order of 0.03 K m/s, while a value of the order of 0.003 K m/s would be typical for the upper surface layer and therefore could be taken in principle for a mountain peak appearing really "suddenly" into the flow. Nevertheless, some concession should be made to surface effects along the slope and therefore the assumed value of 0.009 K m/s. The local temperature gradient is then evaluated from equation (5).

The resulting C_T^2 profile is found in Figure 1 (solid line). Integrating from 5 to 60 m over a vertical line, for a wavelength of $0.5 \mu\text{m}$, a pressure of 770 mb, a temperature of 10° , one arrives at a seeing contribution of 0.13 arcsec, indeed a reasonable value for the near ground contribution.

Expressions (1) to (6) already allow some quick-look conclusions about the dependence of C_T^2 on atmospheric parameters: the most immediate is that either no wind turbulence ($\frac{du}{dz} = 0$), or isothermal conditions ($\frac{d\theta}{dz} = 0$) would mean a zero C_T^2 .

The model shows an almost linear dependence of the near-ground seeing with the turbulent velocity: at the reference mean velocity of 10 m/s, the computed seeing varies from 0.06 arcsec with $\sigma_u = 0.4$ m/s to 0.28 arcsec with $\sigma_u = 1.4$ m/s. With respect to mean velocity the model shows an increase of seeing with lower mean velocities: 0.28 arcsec for $U = 5$ m/s and the typical corresponding average σ_u of 0.65 m/s. However, one should note that at lower mean velocities the range of associated

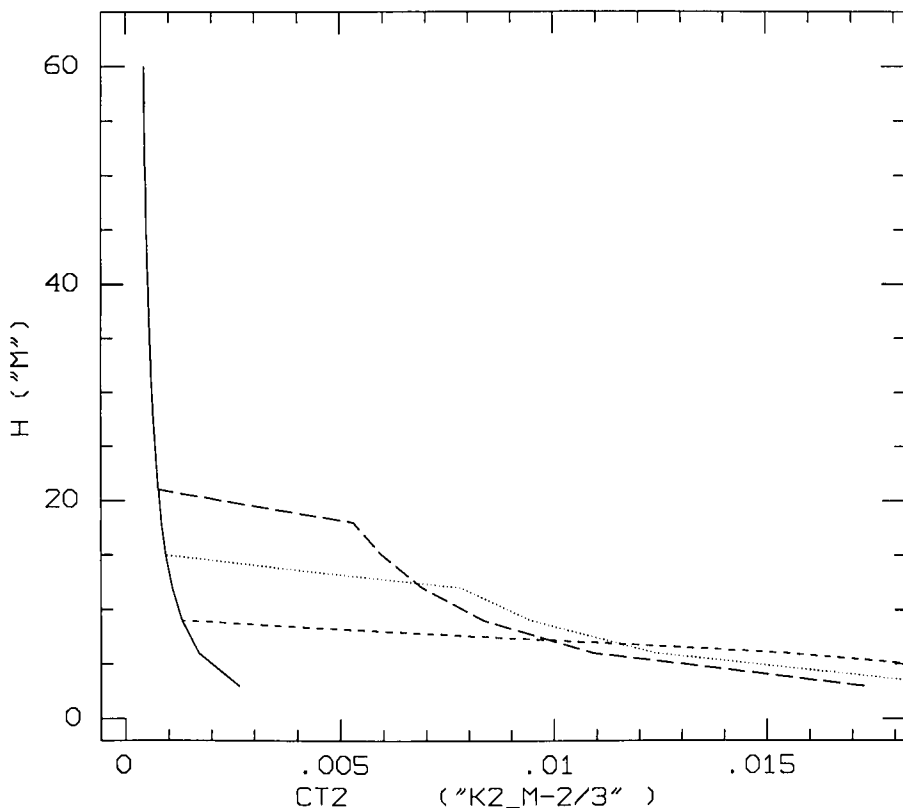


Figure 1: C_T^2 as a function of height for the reference case at the platform edge (solid line) and for distances of 50, 100 and 150 m respectively (dotted lines) from the edge with $z_0 = 0.1$ m and $\Delta\theta_s = 1^\circ$.

turbulent velocities become relatively larger: for instance, again at Paranal, for a mean wind of 5 m/s we record σ_u values from 0.1 to 1.1 m/s, so that, in reality, the model is telling us that at low wind mean velocity one may expect a very large scattering (from very good to very bad) of near ground seeing values.

3. Seeing Along an Extended Platform

We will now apply the simplified C_T^2 model to the case where a hypothetical telescope is not located on the mountain peak or ridge but at some distance from it with respect to the prevailing wind direction. In this case the air flow reaching the telescope's field of view will have already "felt" the ground surface upwind:

- Additional turbulence will be caused by the friction along the upwind surface.
- In the likely case of a temperature difference between the air flow and the ground, the convective heat transfer across the flat surface will modify the temperature distribution with respect to the condition in the incoming flow.

When the undisturbed wind flow meets a flat ridge, the surface stress increases immediately. This sudden increase travels upwards so that one can divide the air flow by a boundary line (see Fig. 2): the flow below this line is

called the internal boundary layer (IBL) and has been affected by the terrain, the flow above has not. From the consideration that the vertical signal velocity should be proportional to the surface stress, the following equation has been derived which links the height δ of the IBL to the distance x from the edge:

$$1 + \frac{\delta}{z_0} \left(\ln \frac{\delta}{z_0} - 1 \right) = kB \frac{x}{z_0} \quad (7)$$

where B is a constant approximately equal to 1.3 and z_0 is the roughness length of the flat surface. Figure 3 shows the evolution of the height δ of the IBL as a function of fetch x , over a length of 200 metres for $z_0 = 0.05$ m, which corresponds to a smooth ground (for instance the runway area of an airport), $z_0 = 0.1$ m (countryside with roads

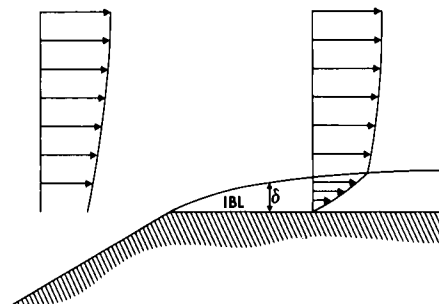


Figure 2: Growth of the internal boundary layer.

INTERNAL BOUNDARY LAYER

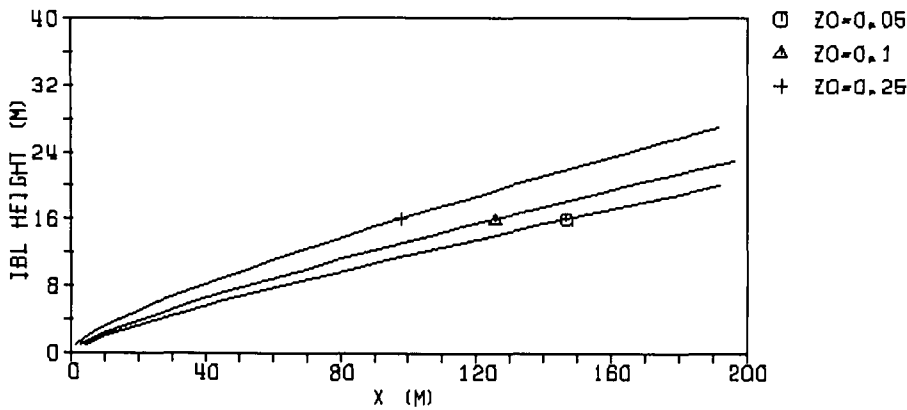


Figure 3: Height of the internal boundary layer as a function of fetch x for different values of roughness length z_0 .

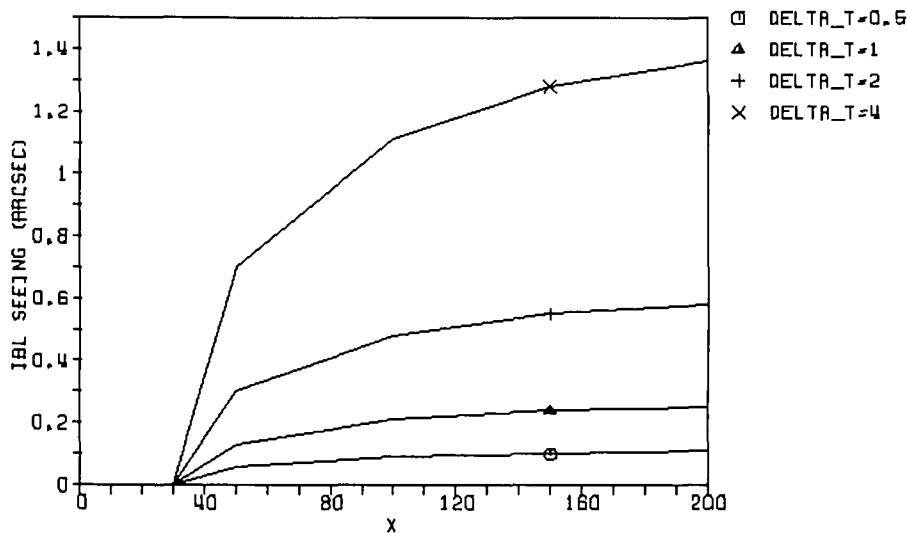


Figure 4: Seeing in the IBL (integrated from 5 m to the top of the IBL along a vertical line) as a function of fetch x for different values of $\Delta\theta_s$. Note that there are no IBL effects until about 30 m from the edge where the height of the IBL reaches 5 m.

and a few hedges) and $z_0 = 0.25$ m (many hedges, a few structures).

Very approximately, velocity profiles below and above δ are logarithmic with different slopes so that a kink appears at δ . From the condition of continuity across the IBL interface one can compute the local friction velocity u_{IBL}^2 , ob-

taining then $\frac{dq}{dz}$ from (4). The vertical heat flux in the IBL is assumed constant and equal to the average air-surface flux:

$$q(z) = q_s = C_H U \Delta\theta_s = \frac{u_{IBL}^2}{U^2} U \Delta\theta_s \quad (8)$$

where $\Delta\theta_s$ is the potential temperature difference between the top of the IBL

and the ground, while C_H is the bulk heat transfer coefficient, here assumed to be equal to the momentum transfer coefficient for a turbulent boundary layer.

One has now all the inputs for a C_T^2 model in the IBL.

Figure 1 shows the vertical C_T^2 profile computed for $\kappa = 50, 100$ and 150 m, assuming $z_0 = 0.1$ m and $\Delta\theta_s = 1^\circ$: the C_T^2 values in the IBL are in this case about one order of magnitude greater than in the free wind flow. However, because of the short integration path, the high C_T^2 does not necessarily result in an unacceptable seeing contribution, as one can see from Figure 4. Only in case of a strong ground cooling, the IBL seeing becomes relatively large.

4. Conclusions

While it should be reminded that the results computed with this simple model of C_T^2 cannot claim any absolute accuracy, it is nonetheless possible to draw some conclusions from the comparison of different situations.

The height and turbulence of the IBL are dependent on the average roughness of the surface, which a good design should therefore try to minimize, by avoiding raised structures and any kind of obstacles likely to contribute to the turbulence generated locally. However, the stronger effect on the IBL seeing will likely be caused by temperature differences between the ground and the incoming flow: this difference will have to be minimized by selecting surface materials which are lightweight and of low conductivity: for instance porous gravel should be used rather than solid rock. In this way the heat flux through the ground will be reduced and the thermal time constant of the surface will be correspondingly decreased.

In a next article, we will discuss the possible seeing effects in the wake of other structures, which is another important aspect of the design of a multi-telescope observatory.

Visiting Astronomers

(April 1–October 1, 1990)

Observing time has now been allocated for Period 45 (April 1–October 1, 1990). The demand for telescope time was again much greater than the time actually available.

The following list gives the names of the visiting astronomers, by telescope and in chronological order. The complete list, with dates, equipment and programme titles, is available from ESO-Garching.

3.6-m Telescope

April: Butcher/Slingerland/Pottasch E./

Baade/Christensen-D./Frandsen, Boulanger/Falgarone/Gérin/Harmon, Ögelman/Gouiffes/Melnick/Augustejjn/Hasinger/Pietsch, Danziger/Bouchet/Gouiffes/Lucy/Wampler/Fransson/Mazzali, Turatto et al. (4-004-45K), Chincarini/Buzzoni/Molinari, di Serego Alighieri/Fosbury/Quinn/Schlötelburg/Tadhunter, Reimers/Koester, Tammann/Leibundgut/Stein.

May: Sackett/Jarvis, Magazzù/Strazzulla, Moorwood/Oliva, Hensberge et al. (5-005-45K), Baade/Crane, Reipurth/Dubath/Mayor, Ehrenfreund/Leger/Foing, Möllenhoff/Madejsky, Bertola et al. (1-008-43K), Shaver, Melnick/Gopal-Krishna/Steppe/Giraud, Danziger/Bouchet/Gouiffes/Lucy/Wampler/Fransson/Mazzali.

June: Leinert/Haas, Perrier/Mariotti/Mayor/Duquenooy, Danziger/Bouchet/Gouiffes/Lucy/Wampler/Fransson/Mazzali, Turatto et al. (4-004-45K), Epchtein/Le Bertre/Blommaert/van Langevelde/Nguyen-Quang-R./Winnberg/Lindquist/Habing, Ferlet/Vidal-Madjar/Dennefeld, Rosa/Mathis, Pottasch S.R./Manchado/Garcia Lario/Sahu K.C.

July: Käufel/Stanghellini/Renzini, Lagrange-Henri/Maillard/Vidal-Madjar/Gry/de Muizon/Ferlet/Beust, Glass/Moorwood/Moneti, Danziger/Bouchet/Gouiffes/Lucy/Wampler/Fransson/Mazzali, Turatto et al. (4-004-45K), Sicardy/Brahic/Barucci/Ferrari/Fulchignoni/Roques, Habing et al. (5-004-45K), Dettmar/Shaw/Klein, Cappellaro/Held/Capaccioli, Held/Cappellaro/Capaccioli, Bertola/de